Toward Sensitive Graphene Nanoribbon-Nanopore Devices by Preventing Electron Beam Induced Damage

Matthew Puster,[† 1,2] Julio A. Rodríguez-Manzo,[† 1] Adrian Balan,[† 1] Marija Drndić[1]*

[1]Department of Physics and Astronomy, University of Pennsylvania, Philadelphia, Pennsylvania,19104.

[2]Department of Materials Science and Engineering, University of Pennsylvania, Philadelphia, Pennsylvania, 19104.

[†]These authors contributed equally to this work.
[*]Correspondence to Marija Drndić email: drndic@physics.upenn.edu

Graphene nanoribbon characterization

Characterization of the fabricated GNRs was performed using atomic force microscopy (Fig. S2), electron diffraction (Fig. S7), and Raman spectroscopy (Fig. S8).

Additional TEM and optical images of the devices and setup

Figures S3, S4, and S5 show additional TEM images of GNRs before and after nanopore drilling, GNRs with side gates and a GNR that was cut to form a nanogap with the nanopore in the center. Figure S6 shows TEM images of a GNR drilled by a TEM method, where the GNR was previously covered with an additional layer of Al_2O_3.

GNR resistances before and after nanopore formation using STEM and TEM methods

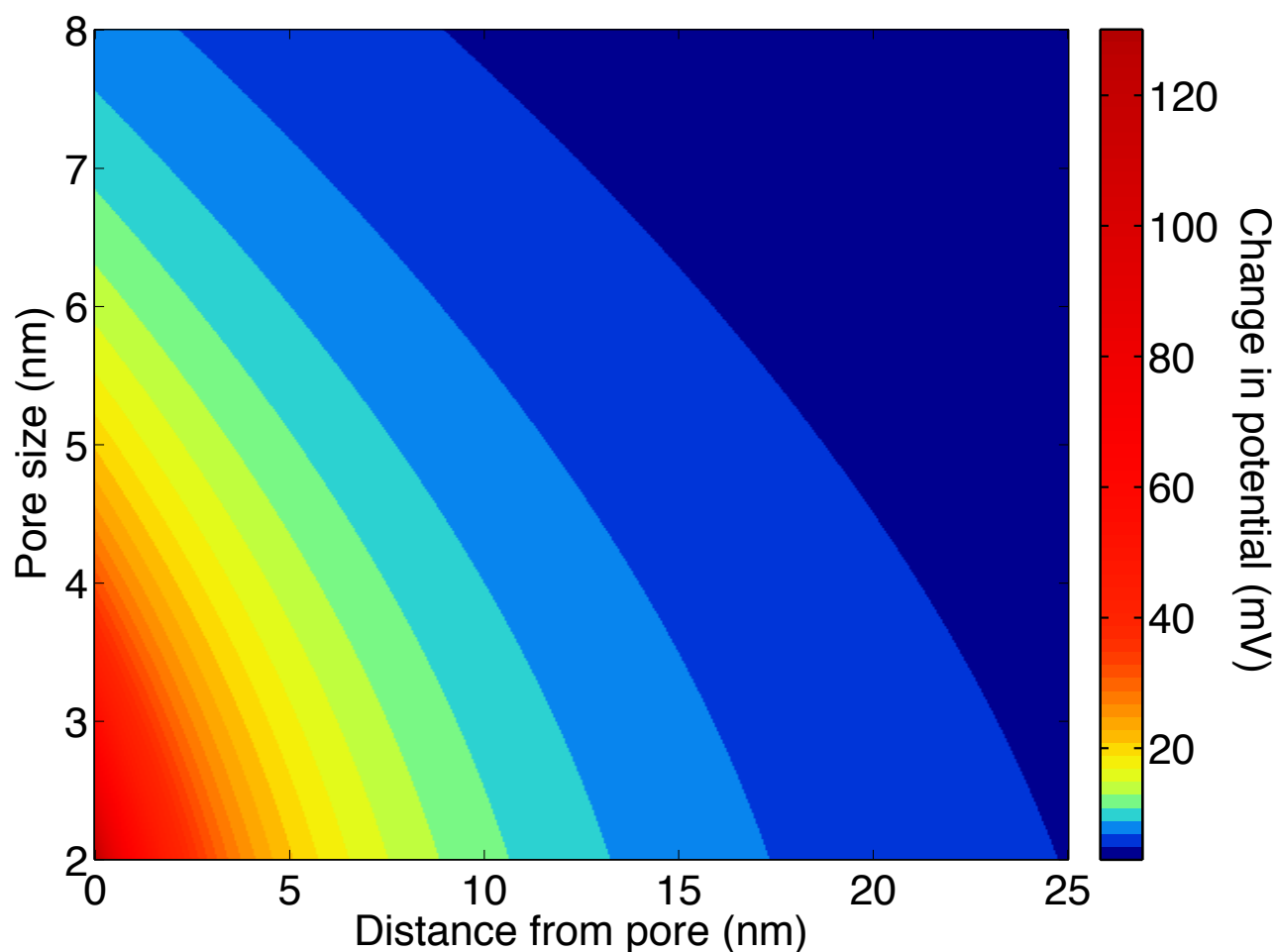Bar graphs of resistances for 22 GNRs drilled using either STEM or TEM methods are shown in Figure S9.

Figure S1. Change in electric potential as a function of distance from the nanopore and nanopore size. Calculation of the change in potential around the nanopore as the DNA translocates through the nanopore, based on the model presented by Xie, *et al*.[16] The potential change is calculated as a function of the distance from the pore and the pore size. The calculation was made for an ionic voltage of 500 mV, a substrate thickness of 50 nm, and a salt gradient of 10 mM KCl in the cis chamber (near the device) and 1 M KCl in the trans chamber.
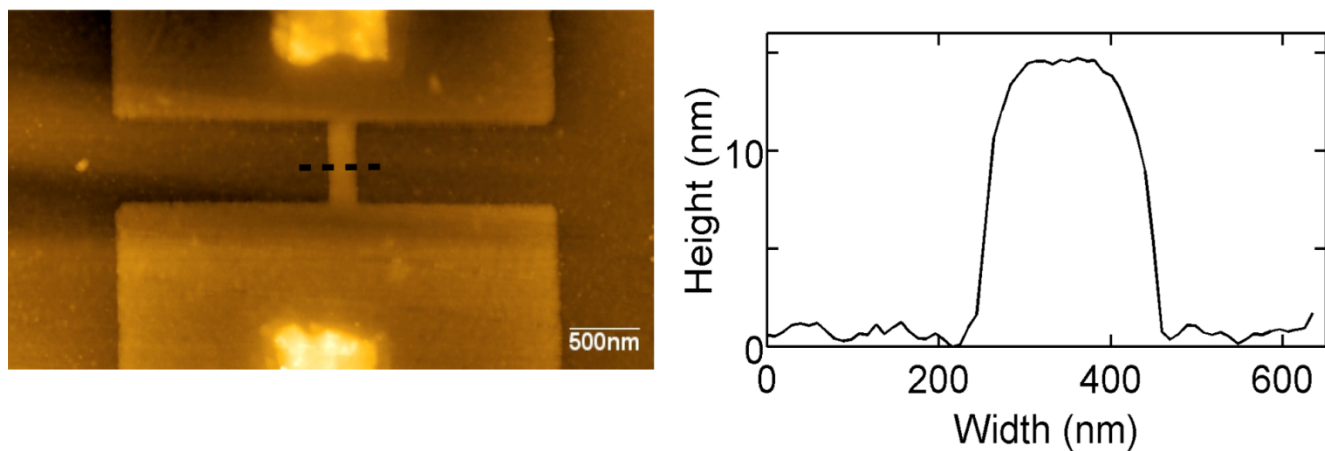
Figure S2. Atomic force microscope image of a GNR. Atomic force microscope image of a ~ 200 nm wide graphene nanoribbon (left) and the corresponding height profile along a black dashed line (right). The HSQ etch mask on top of the GNR has a thickness of ~ 15 nm.
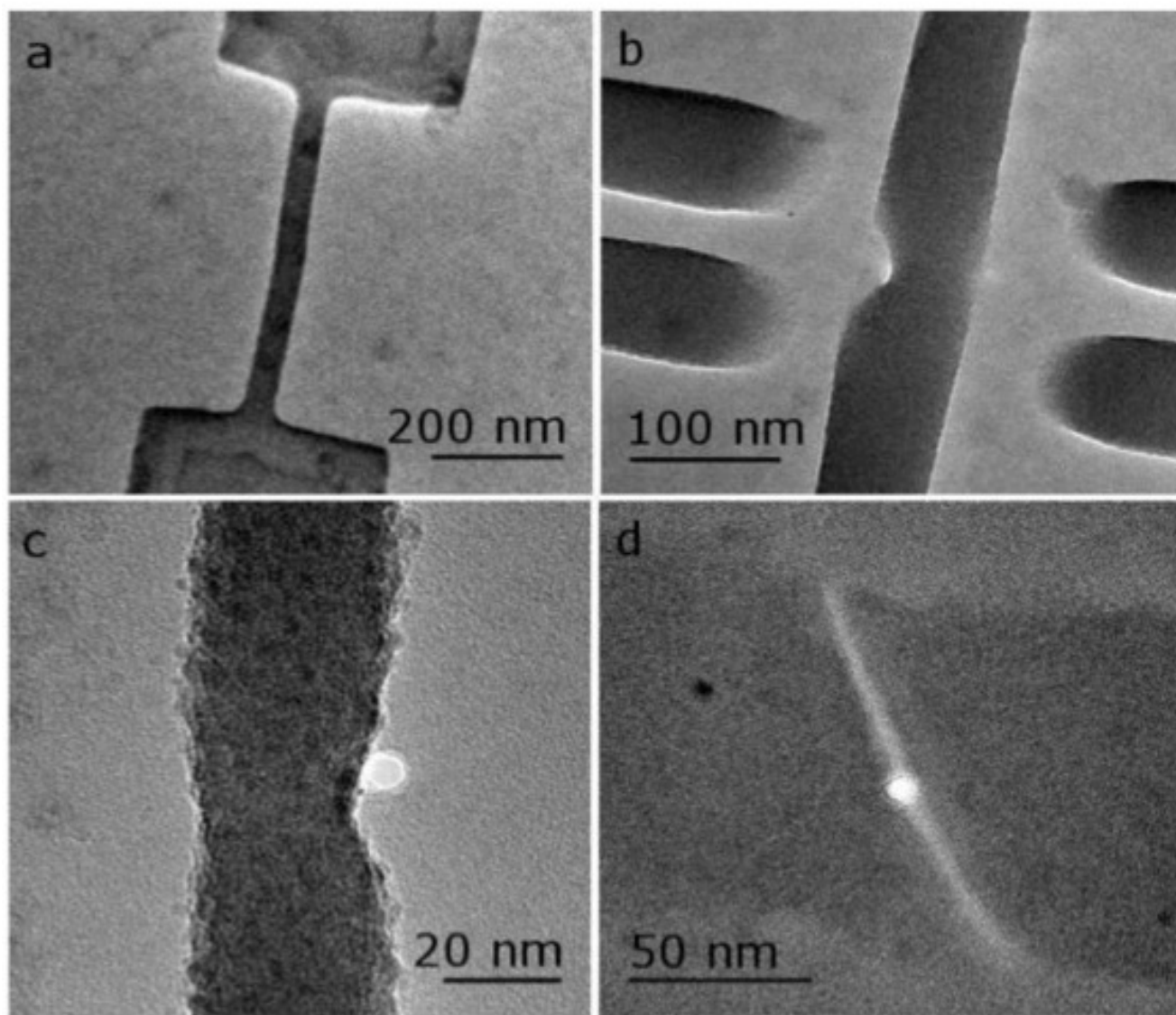
Figure S3. Additional TEM images of GNR and GNR-NP devices. (a) 40 nm wide GNR with HSQ etch mask. (b) 50 nm wide GNR with side gates. (c) 20 nm GNR with NP. (d) TEBAL-cut 100 nm GNR with a 3 nm nanogap and a 7 nm diameter NP in the center.
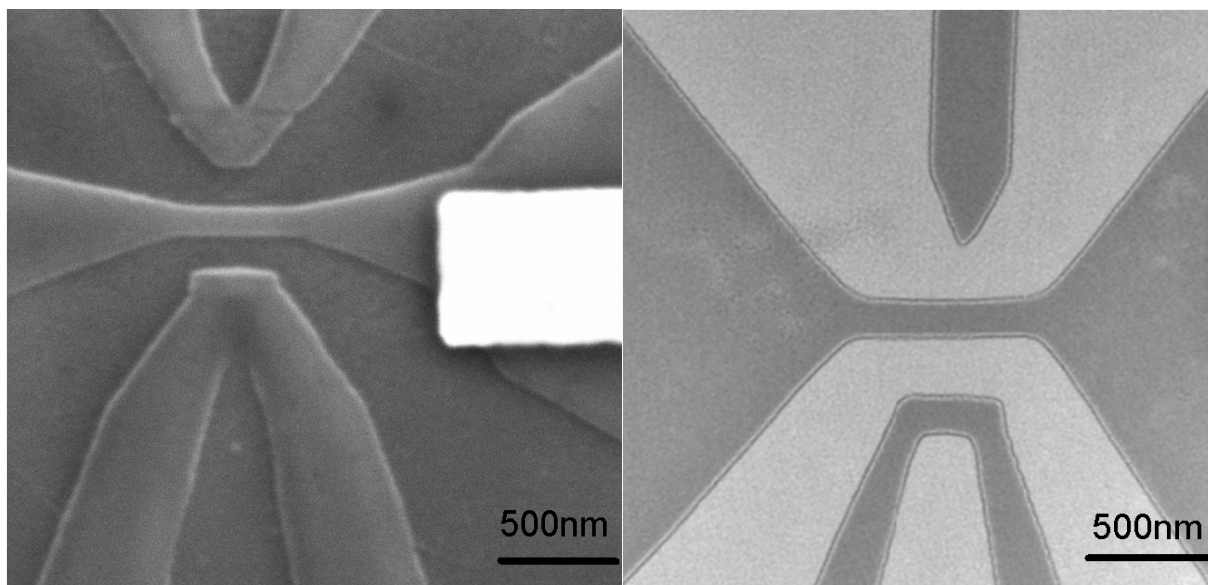
Figure S4. Side-gated GNR devices. SEM (left) and TEM (right) images of side-gated GNR devices. The side-gate can be used to shift the Fermi level of the GNR to a level of maximum sensitivity to the external potential change, (dR/R)/dVg.
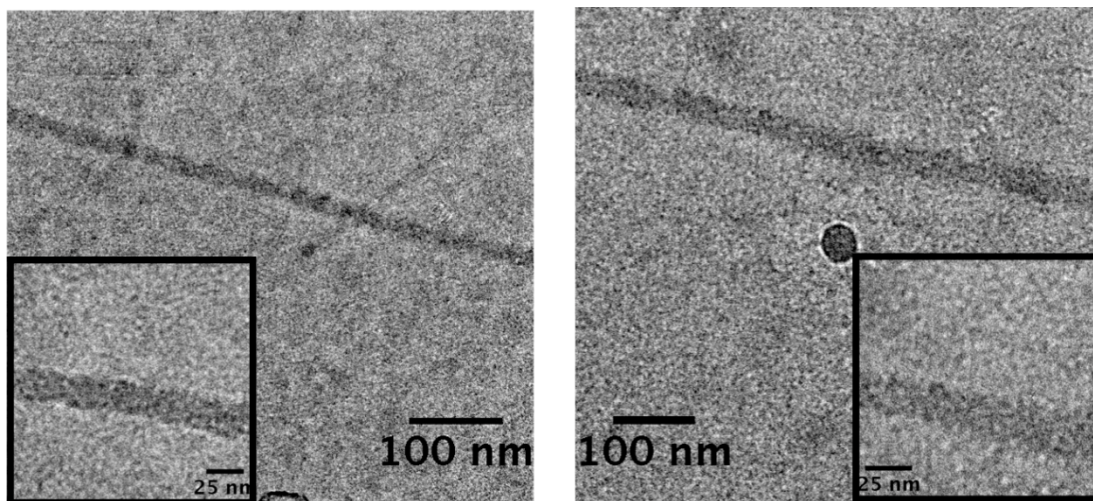
Figure S5. 20 nm wide GNRs. Additional TEM images of 20 nm wide GNRs on SiN$_x$ windows, covered with the HSQ etch mask.
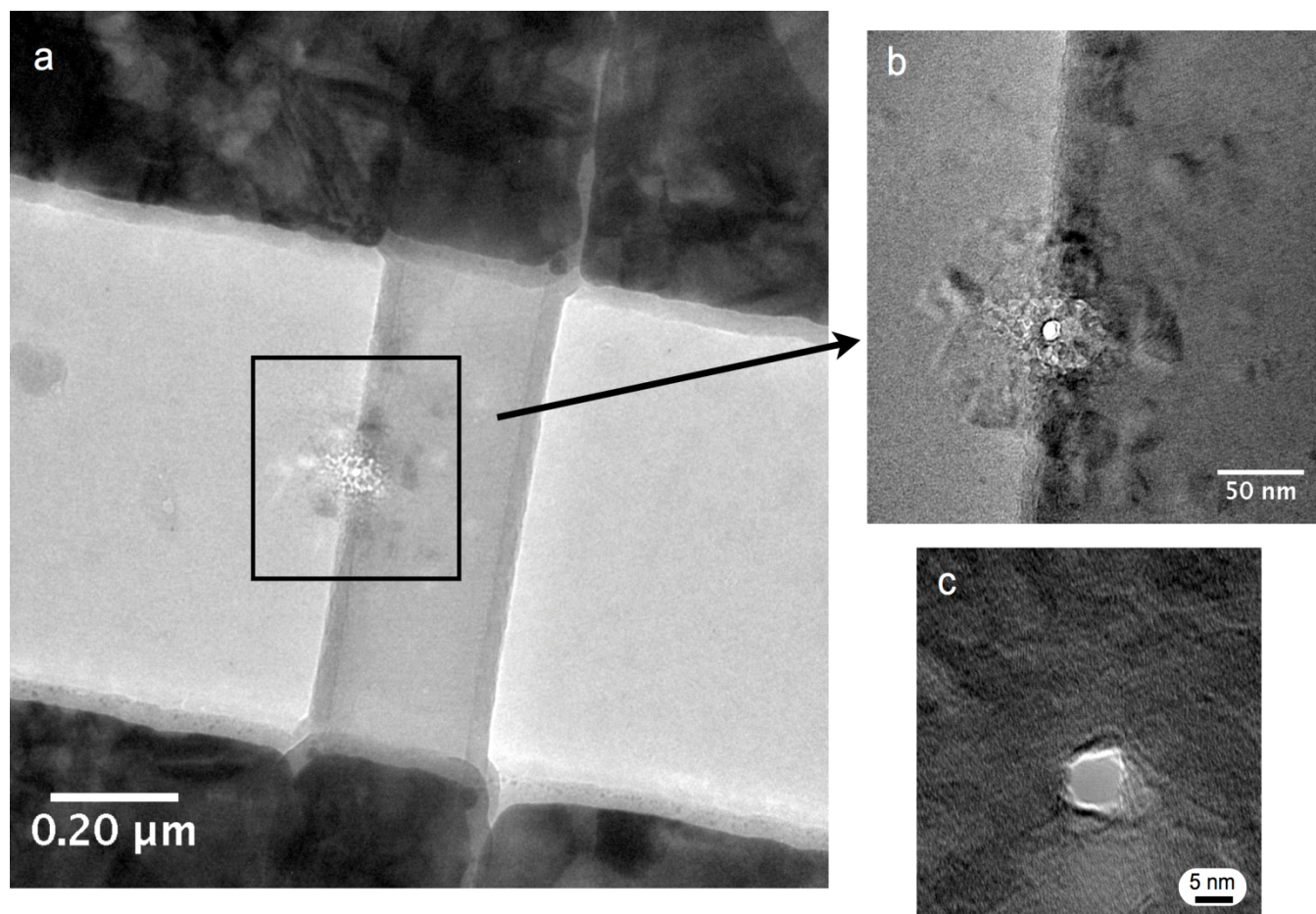
Figure S6. Beam-induced damage in a GNR-NP device covered with an Al₂O₃ layer. TEM images at various magnifications (a-c) of one GNR-NP device that was coated with a 20 nm Al$_2$O$_3$ layer grown by atomic-layer-deposition (ALD) and then drilled in TEM mode to form a nanopore at the edge of the GNR. The circular area around the NP where material is damaged is indicated by the black square in (a) and is clearly visible in (b). The damage extends ~ 100 nm from the nanopore (c) shows the zoom in of the NP.
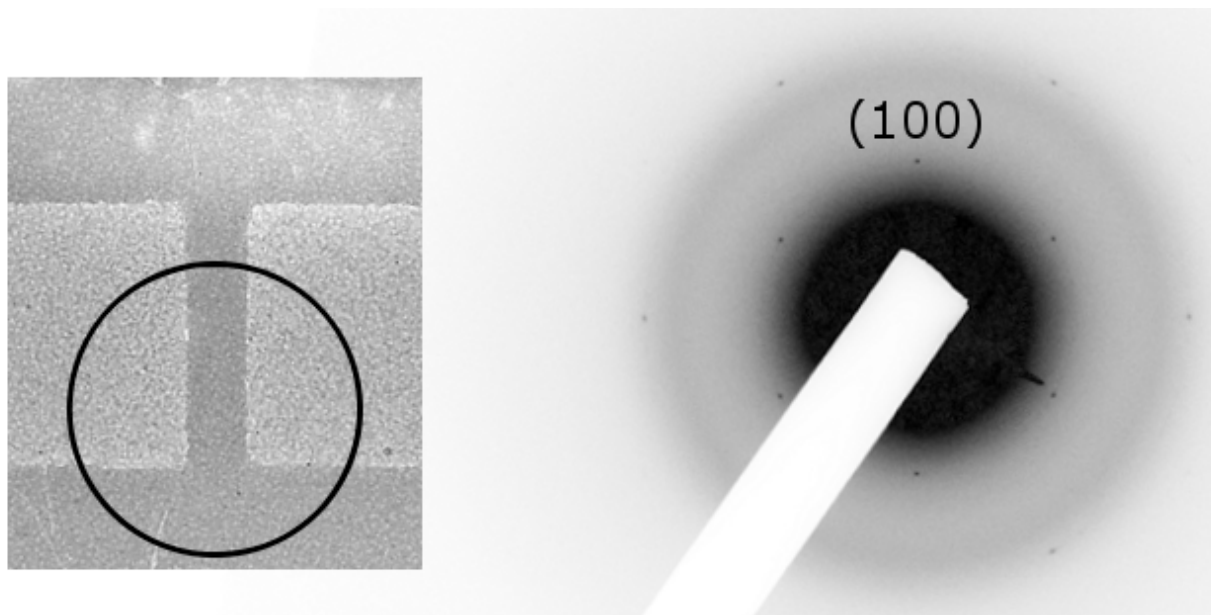
Figure S7. **Electron diffraction pattern of a GNR**. The right panel shows the electron diffraction pattern taken from a 1 μm diameter area of a GRN (indicated by the black circle in the left panel). The signal of the spots (e.g. (100)) is weak because of the background contribution of the HSQ and the SiN_x membrane.
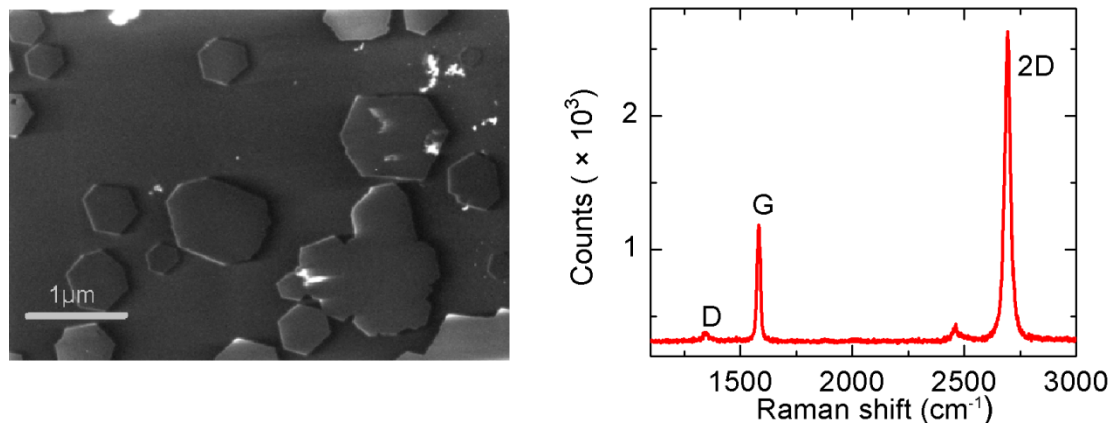
Figure S8. **Transferred CVD-grown graphene and Raman characterization**. Left panel shows a SEM image of graphene hexagons grown by CVD and transferred to a SiN_x window, proving the ability to control the coverage rate in our growth process. For our devices we opted for a continuous film for processing reasons. The right panel shows a Raman spectra of a representative graphene film after transfer to a SiO_2 substrate. The shape of the 2D peak (with a full with and half maximum of 30 cm^{-1}) and the relative high intensity of the 2D peak (2700 cm^{-1}) with respect of the G peak (1588 cm^{-1}) confirms that we have single layer graphene. The low intensity of the D peak (1350 cm-1) proves the high quality of our transferred graphene monolayer films.
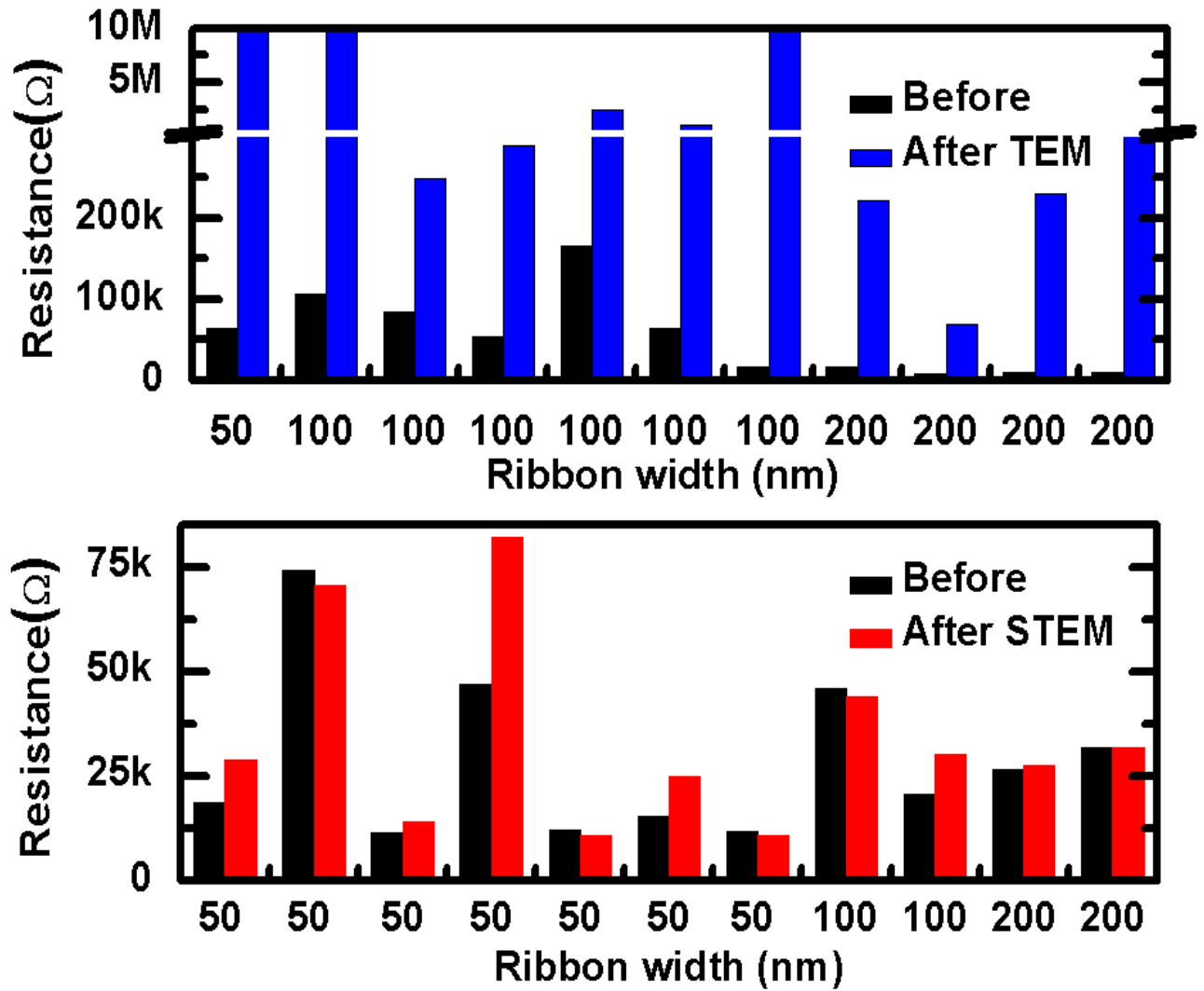
Figure S9. Bar graphs of GNR resistances. Bar graphs of individual GNR resistances for 22 devices before and after nanopore drilling in the TEM method (top bar graph) and STEM method (bottom bar graph). The black bars correspond to GNRs before drilling, and the blue and red bars correspond to TEM and STEM-drilled devices, respectively. The x-axes in both bar graphs indicate the nominal width of the GNR. All 50 nm and narrower GNRs exhibit ~ GΩ resistance after TEM drilling. For 100 to 200 nm wide TEM-drilled GNRs, the resistance increases by one or more orders of magnitude. In contrast, for all the STEM-drilled GNRs regardless of width (bottom histogram), the GNR resistances before and after nanopore formation remain the same on average.
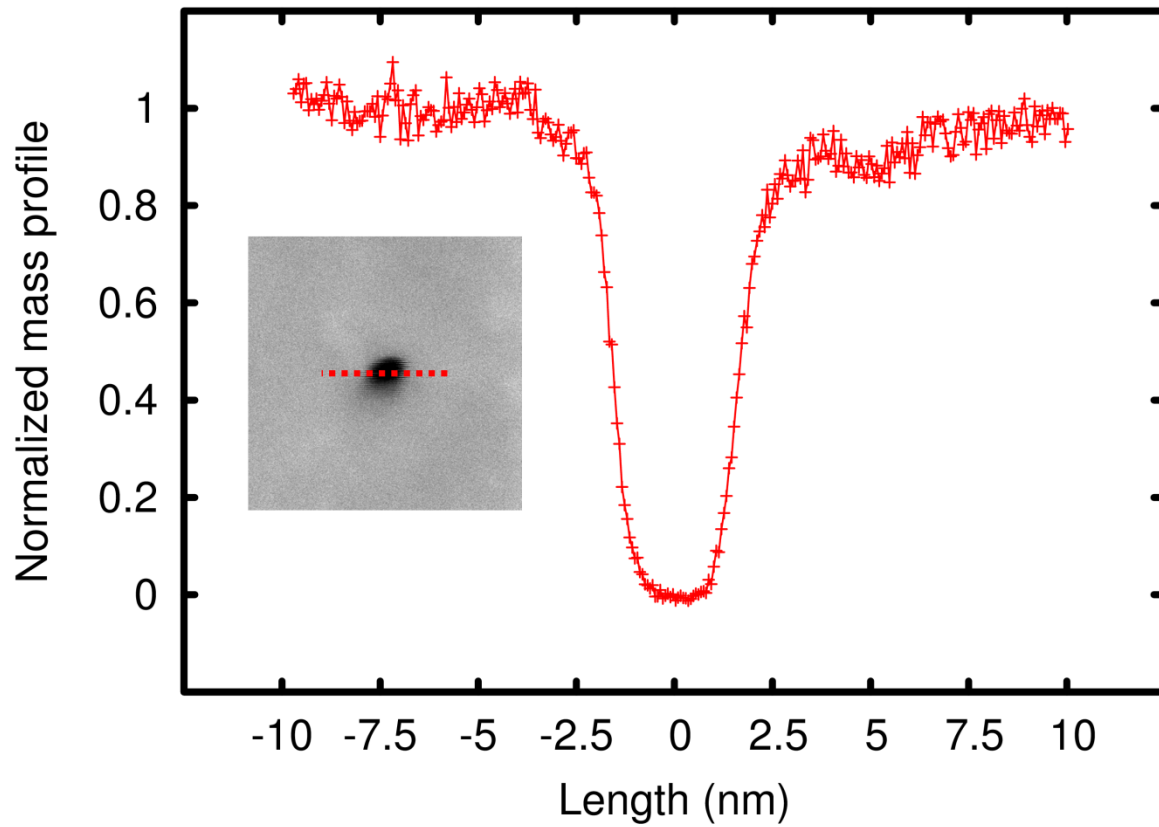
Figure S10. Mass profile of a nanopore. Mass profile from a HAADF STEM image of a nanopore made in a 40 nm thick SiN_x membrane made. The nanopore was made with a beam diameter of 2.4 nm and a dose of 5×10^{10} C m^{-2}. From the mass profile we measure a nanopore diameter of 2 ± 0.3 nm for this particular nanopore. The HAADF STEM image was acquired with a 0.3 nm beam.